Modeling, Control and Laboratory Testing of an Electromagnetic Docking System for Small Satellites

Article *in* Advances in the Astronautical Sciences · January 2020

3 authors:


Aaditya Ravindran
Arizona State University


Leonard Vance
The University of Arizona


Jekan Thangavelautham
The University of Arizona

MODELING, CONTROL AND LABORATORY TESTING OF AN ELECTROMAGNETIC DOCKING SYSTEM FOR SMALL SATELLITES

Aaditya Ravindran,* Leonard D Vance,† and Jekanthan Thangavelautham‡

Small-satellites and CubeSats offer a low-cost pathway to perform technology demonstrations in space, deploy instruments for earth observation and perform exploration. Small-spacecrafts and CubeSats have the potential to be modules that can be constructed into large structures and observatories in space. This would require small-spacecraft and CubeSats to have mechanisms to dock. Such an approach avoids high-risk due to a single launch failure or loss of an individual craft. The CubeSat or small-spacecraft modules maybe stockpiled from many launches. Various docking mechanisms like the Power Data Grapple Fixture (PDGF) on the ISS and the Soyuz docking system have been developed. Small satellite docking mechanisms are just emerging. This paper proposes development of a general purpose electromagnetic docking mechanism. This electromagnetic docking mechanism is an example of a nonlinear system. The dynamics of the system is modeled. Using this dynamics model, various controllers have been designed. The selected controller has a distance-controlled feedback loop to perform docking. A preliminary mission concept to test the docking mechanism and the docking controller has been proposed and discussed. A prototype of a docking system is evaluated in the laboratory and discussed in the paper.

INTRODUCTION

The need for interplanetary travel and exploration has encouraged plans to build in-space human habitats [24], communication relays [23], and fuel depots. The Hubble Space Telescope (HST) (Figure 1) is a large space structure that forever changed astronomy. The infamous defective mirror of the HST almost resulted in the end of mission [2]. At various times in the life of the HST, it had defective computers and gyros [3]. Various servicing missions helped to prolong the life of the HST and to repair and replace defective components. In-space servicing and repair salvaged this critical mission.

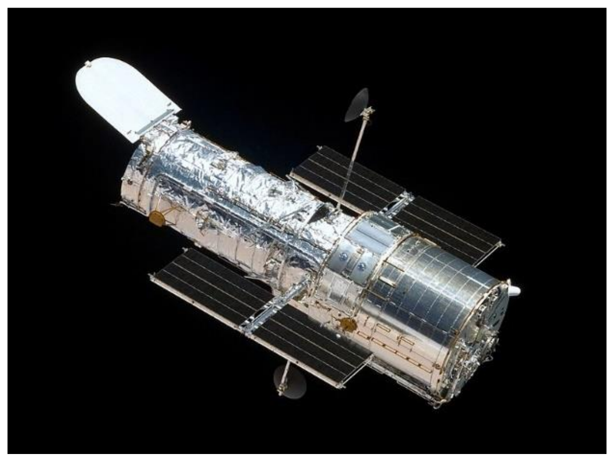

Figure 1: Hubble Space Telescope (courtesy of NASA).

The International Space Station (ISS) is another example of a large space structure and is considered the largest one to date. The ISS was built over a course of 13 years, starting from 1998 to 2011 [4], and is continuing to get new modules and components. Modularity was the key to building the ISS. The key to modularity was ability to interconnect major modules and rearrange them if needed. State-of-the-art docking systems include the Power Data Grapple Fixture (PDGF)

* SpaceTREx Laboratory, Arizona State University, Tempe, AZ 85281, aravin11@asu.edu.
† SpaceTREx Laboratory, University of Arizona, 1130 N Mountain Ave, Tucson, AZ 85721, ldvance@arizona.edu
‡‡ SpaceTREx Laboratory, University of Arizona, 1130 N Mountain Ave, Tucson, AZ 85721, jekan@arizona.edu

for non-pressurized payloads (Figure 2) and the Soyuz docking system for living modules. The PDGF costs more than 2 million US dollars, and on top of that docking maneuvers are performed by highly skilled astronauts. Docking is a dull task and such a system is prone to human errors. One such incident was the docking of a Progress module to Mir space station in 1997 [5]. It is therefore essential that docking system is reliable and not prone to human errors. An automated docking system is a credible alternative.

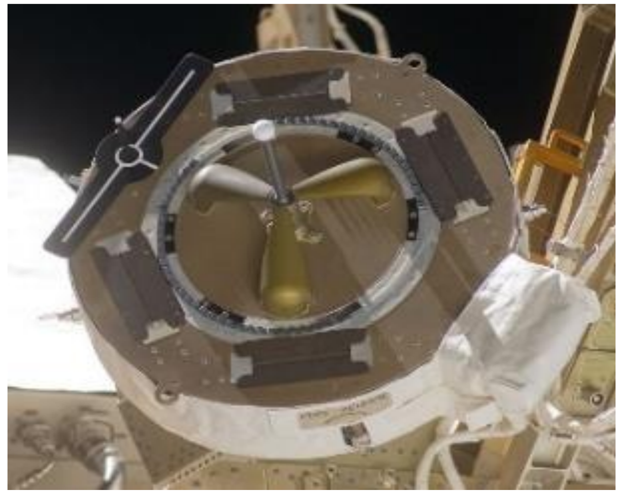

Figure 2: Power and Data Grapple Fixture (NASA)

Docking systems which have been developed and deployed so far have been for large satellites and structures. Some small satellite docking systems have been developed and ground tested but have yet to be demonstrated in space. It is therefore critical that various low-cost autonomous docking system designs are developed and tested on small satellites in space.

Developing such autonomous docking systems not only will enable in-space assembly and repair, but also reduce or eliminate humans out of the loop. These systems will not only be able to perform self-assembly, but also share resources, like power, data, and possibly fuel. This paper focuses on modeling of an electromagnetic probe and cone docking mechanism for CubeSats. By going small and autonomous, we intend explore the use of CubeSats to perform in space assembly of large space structures and instruments. In our approach, we devise several candidate control systems and apply them to the problem at hand. Our results show that an autonomous approach to docking is possible without the need for bulky cameras or humans in the loop. In the following sections, we first present related work, followed by approach and an example mission concept that applies this proposed technology. In the results sections, we present detailed simulation of two 3U CubeSats docking and analysis of the docking controller. This is followed by laboratory experiments to validate our electromagnetic docking technology. Finally, we present conclusions and future work.

RELATED WORK

Docking mechanisms which have been designed are variations of probe and cone, also called probe and drogue. These are either used for berthing or data and power transfer. These docking systems for berthing the ISS have been developed and tested for big spacecrafts like for the Gemini, Apollo, Soyuz (Figure 3), [6]. The PDGF is used by Canadarm2 on the ISS to grapple objects and manipulate by powering them and performing data transfer.

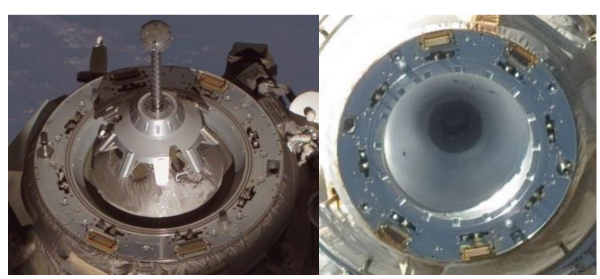

Figure 3: Soyuz Docking System (courtesy of NASA).

Some of the small satellite docking mechanisms have been designed and ground tested have not been space tested. Various missions demonstrating small satellite docking are discussed below.

AAReST Mission

Underwood et al. [7] have proposed a CubeSat mission to demonstrate the concept of Auton omous Assembly of Reconfigurable Space Telescope (AAReST). The mission proposes a 15U CubeSat which will demonstrate in-space assembly of the MirrorSats (Figure 4). To perform in-space assembly, the rendezvous and docking system has been designed as a probe and cone docking system with electromagnets and attitude control strategies for coarse docking, a Microsoft Kinect based array of sensors, LIDAR and Camera RDV sensors, a differential GPS for relative navigation. The authors have described tests that have been performed to dock the cubesats using the electromagnetic docking mechanism. According to Eckersley et al. [8], the AAReST mission is set to be launched in 2018 or later.

Figure 4: MirrorSats of the AARST Mission (courtesy of [8]).

CPOD Mission

Bowen et al. [9] have proposed a Cubesat based rendezvous, Proximity Operations, and Docking (CPOD) mission, previously known as the Proximity Operations Nano-Satellite Flight Demonstrator, PONSFD [10] solely to test small satellite docking. They propose the use of a Universal Docking Port (UDP) [11], a semi-androgynous docking mechanism used in SPHERES [12]. The CPOD mission proposes 4 docking sensors in the Remote Proximity Operations and Docking (RPOD) module (Figure 5) which are, near and wide field visible range cameras and near and wide field IR cameras. This mission is said to demonstrate the capability of the UDP. According to the authors, the CPOD mission is also set to launch in 2018 or later.

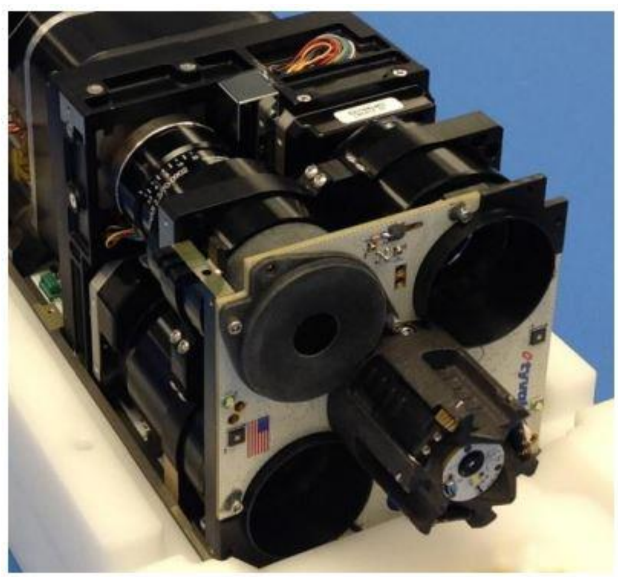

Figure 5: RPOD Module of the CPOD Mission (courtesy of [9]).

ARCADE-R2 Mission

Barbetta et al. [13] have proposed an Autonomous Rendezvous, Control, and Docking Experiment - Reflight 2 (ARCADE-R2). This mission was proposed as a technology demonstrator experiment to prove the feasibility of small satellite docking. On October 10, 2013, it flew on board the BEXUS-17 stratospheric balloon, successfully performing the docking procedures. The docking system (Figure 6) design is again based on a probe and cone system with IR LEDs and IR LDR sensors to assist in the docking. The actuation was performed using the on-board attitude control system.

Other Missions

Pei et al. [14] have proposed an autonomous rendezvous and docking system using permanent magnet docking mechanism. The mission acts as a technology demonstrator for a permanent magnet docking mechanism. The authors propose an attitude and position control using relative position navigation with the help of Continuous Differential GPS (CDGPS) and the on-board Attitude Determination and Control System (ADCS).

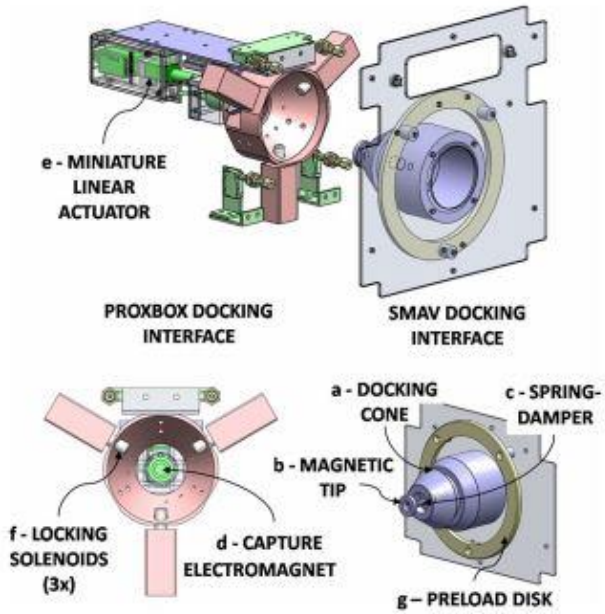

Figure 6: Docking System of the ARCADE-R2 Mission (courtesy of [13]).

The Universal Docking Port [11], designed for the SPHERES facility on-board the ISS is a semi-androgynous docking port designed to provide data and power transfer. The authors describe in detail the complete docking system design and its testing on the SPHERES facility on the ISS. The UDP uses a camera sensor to perform docking in space and has been tested on the SPHERES robots, which are three flying satellites used to test algorithms or other systems. The SPHERES facility with the UDP has also been tested by Miller et al. [15], who proposed an experiment to perform Assembly of a Large Modular Optical Telescope (ALMOST), which was tested while on-board the ISS.

McCormick et al. [16] propose a robotic manipulator with probe and cone end effectors to demonstrate docking of small satellite clusters. Ye et al. [17] propose a docking controller integrated with the attitude control system for the probe and cone docking system and discuss the modeling of forces. Zhang et al. [18] also discusses the force modeling of a probe and cone docking system.

Mission Comparison

The AAReST mission uses electromagnetic docking system, but with bulky sensors which are based on a Kinect camera sensor system and hasn't been tested in space yet. The CPOD mission uses just a probe and cone docking mechanism, with 4 cameras sensors and an integrated attitude controller strategy and hasn’t been tested in space yet. And the ARCADE-R2 mission used just a probe and cone docking mechanism, with IR LEDs and IR LDR sensors and an integrated attitude controller strategy, but only been tested in the upper atmosphere, but not in space.

ARX Model for Electromagnetic Levitation

Qin et al. [19] propose modeling an electromagnetic levitation system as a Gaussian Radial Basis Function (RBF) Autoregressive (ARX) model. The authors discuss a controller based on neural networks for the electromagnetic levitation system with a PID controller to control the identified system.

Feedback Linearization of Electromagnetic Levitation Systems

Gandhi et al. [20] and Romero et al. [21] discuss a comparison of feedback linearization of electromagnetic levitation systems and design of various controllers to maintain the ball levitation system in a suspended state.

APPROACH

The approach is divided into 3 main phases. First, the Attitude Controller, which performs coarse positioning of the docking system. Second, the Docking System Modeling, which deals with deriving the system model for an electromagnetic docking system. Third, the Fine Docking Controller Design, which performs the fine docking of the two small satellites.

Attitude Controller

The Attitude Determination and Control System (ADCS) of the satellite is responsible for 3-axis stabilization and coarse position control of the satellite, which implies that it requires a propulsion system.

Coarse position control of the satellite can be split into orbital maneuvering and docking alignment. Let us consider Satellite A, with the probe part of the docking system and Satellite B, with the cone part of the docking system, as the two CubeSats which will be used in the docking demonstration. When these small satellites are deployed, they can have a large initial separation between them. For the fine docking mechanism to take over, the ADCS will have to perform orbital maneuvering such that the two satellites will be close enough for the docking controller to kick in. Once orbital maneuvering is performed, the satellites need to align themselves so that the docking system on both the satellites will be aligned and reduces the two-dimensional Euclidean distance to one dimension.

This paper assumes that the attitude controller has been designed to perform coarse positioning. However, an experiment proposal is discussed.

For such a demonstration, consider two robotic arms capable of simulating the attitude control system integrated with a docking controller. The end effectors of these two robotic arms represent the two small satellites. The robotic arm representing Satellite A will have a smart camera system capable of detecting and tracking the end effector of the other robotic arm representing Satellite B. This can be used to simulate docking as well. A previous work [22] on smart camera system has demonstrated simulated entry event tracking capabilities (Figure 7).

Docking System Modeling

The Electromagnetic Docking System used can be modeled as a levitation system, based on a

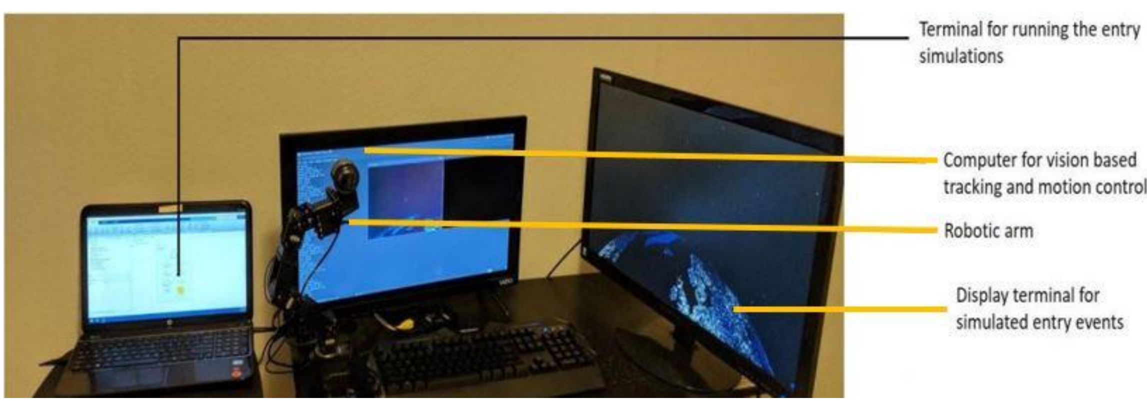

Figure 7: Smart Camera System.

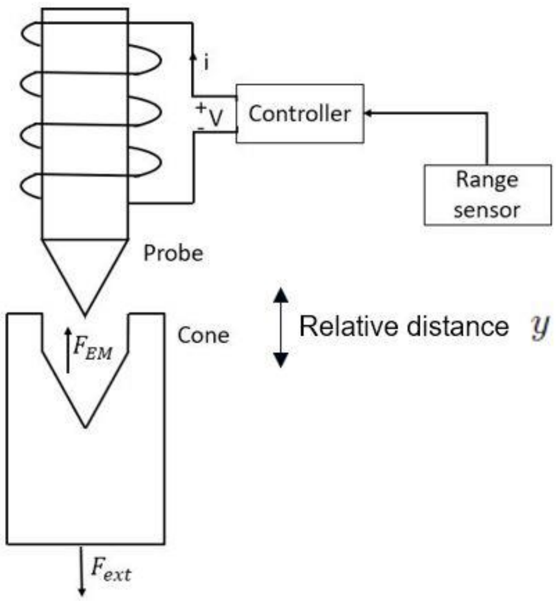

Figure 8: Electromagnetic Docking System Diagram.

probe and cone docking mechanism (Figure 8). This system can be formulated from first principles, using the equation for current (Equation 1) in the probe system and the equation for force (Equation 2) in the cone system.

$$\frac{di}{dt} = \frac{1}{L_1} V - \frac{R}{L_1} i \tag{1}$$

$$\frac{d^2y}{dt^2} = -\frac{F(y,i)}{m} + \frac{F_{ext}}{m} \tag{2}$$

$$F(y,i) = k\left[\frac{i(t)}{y(t)}\right]^2 \tag{3}$$

where i is the current in the electromagnetic coil, V is the applied voltage, R is the resistance of the electromagnetic circuit, $L_1 = \frac{N^2}{Rl}$ is the self-inductance of the electromagnetic coil, N is the number of turns of the electromagnetic coil, Rl is the reluctance of the electromagnetic circuit, y is the relative distance between the probe and cone, F_{ext} is the external force, either gravitational or other forces, and $k = \frac{\mu_0 N^2 A}{l}$ is a constant, where μ_0 is the permeability of free space, A is the effective area of the solenoid core of the probe influencing the cone, l is the length of the coil, m is the mass of the satellite.

Docking Controller Design Outline

This system can be represented in state-space form (Equation 4), with the states $\boldsymbol{x_1 = y, x_2 = \dot{y}, x_3 = i}$, the output as $\boldsymbol{y = x_1}$, and the input as $\boldsymbol{u = V}$.

$$\begin{aligned} \dot{x}_1 &= x_2 \\ \dot{x}_2 &= -\frac{k}{m}\left[\frac{x_3}{x_1}\right]^2 + \frac{F_{ext}}{m} \\ \dot{x}_3 &= -\frac{R}{L_1} x_3 + \frac{1}{L_1} u \end{aligned} \tag{4}$$

The docking controller is responsible for fine docking the two small satellites, from a given separation. To achieve this, multiple controller designs are discussed, compared, and a final controller is chosen to complete the task.

Taylor Series Linearization and Controller Designs

The electromagnetic docking system, is highly nonlinear, as seen from the state-space representation in Equation 4. Hence, to control this nonlinear system, it must be linearized. We first look at the most common type of linearization, the Taylor Series Linearization. This assumes that the system is linear around a small range of states around the equilibrium point given by Eqn 5.

$$x_e = \left[d, \quad 0, \quad d\sqrt{\frac{F_{ext}}{k}} \right]^T$$

$$\text{and, } u_e = Rd\sqrt{\frac{F_{ext}}{k}} \qquad (5)$$

After Taylor Series Linearization, various controller designs based on Bandwidth and Robustness Controller Design, PID controller, and Linear Quadratic Gaussian (LQG) controller design can be performed.

Using Bandwidth and Robustness controller design, it is possible to compute a controller for a particular structure using the closed loop bandwidth of the controller-plant system and the phase margin of the open loop system. With PID controller, it is possible to design a controller by tuning its proportional, integral, and derivative gains. LQG is a controller which is a combination of Linear Quadratic Regulator (LQR) and the Kalman Filter (KF), which is designed to be a robust and some special properties like guaranteed stability.

It is observed that both Bandwidth and Robustness design, as well as PID controller designs, will tend to be unstable, and require intense tuning of the bandwidth in the former case and intense tuning of the PID parameters in the latter case. However, the LQG controller design leads to a stable system. It is seen that the performance of the actual nonlinear system differs from the linearized system drastically, which renders the actual controller unstable. A more detailed explanation can be found in the results section.

Feedback Linearization and Controller Design

Since Taylor Series Linearization doesn't give us usable results, Feedback Linearization can be performed. This type of linearization transforms the nonlinear states and input into linearized states and a new input such that the input-output relation becomes linear as shown in Equation 6.

MISSION CONCEPT

A docking system for small satellites is incomplete without an accompanying mission concept and application. Hence, this section proposes a possible mission concept and how the docking system interfaces with the rest of the satellite.

Mission Statement

The mission consists of two 3U Cubesats to demonstrate the electromagnetic docking system along with the fine docking controller and the coarse positioning system, aimed at advancing the

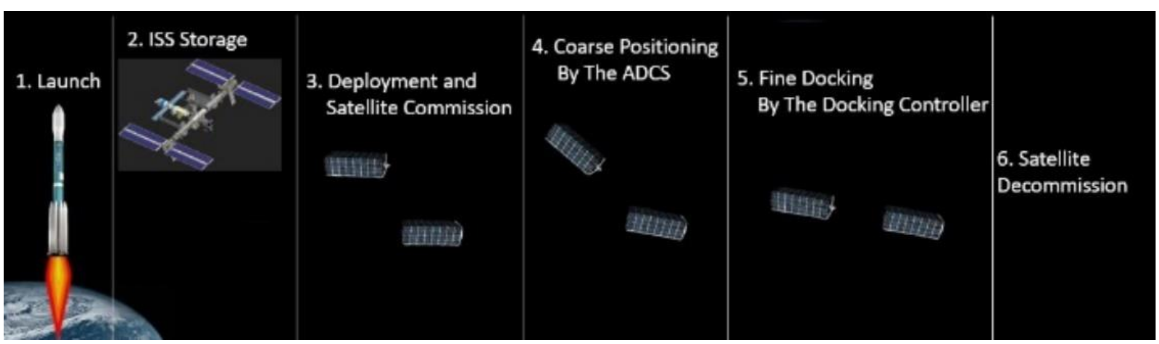

Figure 9: Concept of Operations

capabilities of future in-space assembly and repair missions. Table 1 shows the mass budget.

Concept of Operations

The system will consist of Satellite A, with the probe unit and Satellite B, with the cone unit of the docking mechanism. The mission has two main phases in its operations (Figure 9), namely, the coarse positioning phase where the ADCS performs orbital maneuvers and orients the satellite for the fine docking controller to take over, and the fine docking phase where the fine docking controller performs docking of the satellites followed by data and power transfer checks. Information about the complete docking procedure is then downlinked to the ground station so that docking procedures are verified, and improvements can be made.

System Architecture

The docking system is a two-part system where one unit is the probe unit, which is installed on Satellite A and the other is the cone unit, which is installed on Satellite B. Both the units will be equipped with a data and power transfer port used post-docking. The probe unit of Satellite A will be electrically interfaced with the docking controller and the command and data handling system computer, and mechanically mounted onto the CubeSat structure as shown in Figures 10 and 12.

Table 1: Mass Budget of each Cone/Probe CubeSat

Subsystem	Component	No.	Mass (g)
C&DH	Space Micro CSP	1	40
Communications	Gommspace Nanocom ANT 430 UHF antenna	1	18
	AstroDev Lithium L1 UHF radio	1	30
ADCS	MAI Sun Sensors	6	186
	MAI 400 3 axis RCS	1	694
Power	Gommspace Electrical Power System	1	43
	Gommspace Battery	1	365
	Solar Panels	4	280
Docking system	Electromagnetic Docking System	1	1000
Structure	Chassis	1	500
		Total	3156

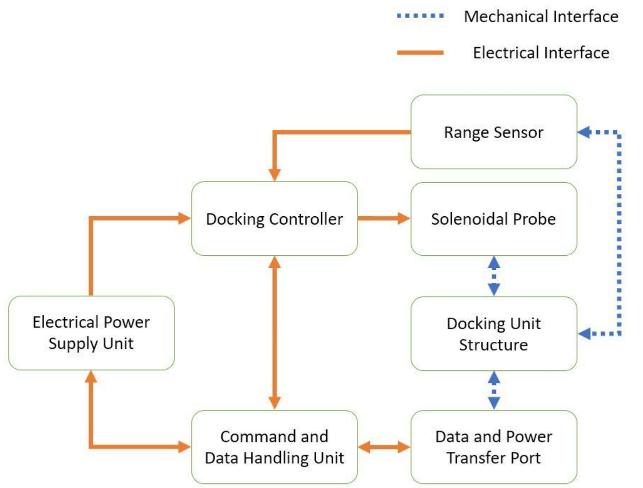

Figure 10: Satellite A (Probe) System Interface Diagram.

The cone unit of Satellite B is a simpler system, which acts as a passive device, which interfaces with the command and data handling system only for data and power transfer after docking (Figure 11, 12).

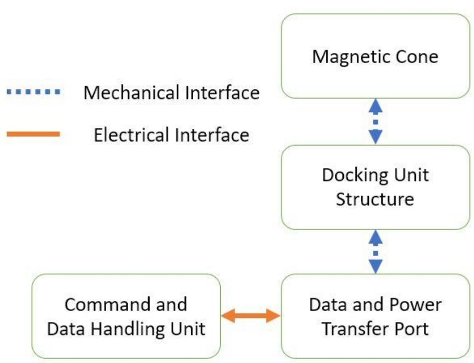

Figure 11: Satellite B (Cone) System Interface Diagram.

Both the coarse positioning system and the docking controller are present in the probe unit, which is considered as an active unit, and the cone unit is considered a passive unit.

The cone unit of Satellite B is a simpler system, which acts as a passive device, which interfaces with the command and data handling system only for data and power transfer after docking (Figure 11, 12). Both the coarse positioning system and the docking controller are present in the probe unit, which is considered as an active unit, and the cone unit is considered a passive unit.

SIMULATION RESULTS

This section describes the results of the controller design, provides a comparison of various controller designs, and illustrates the simulation of the docking system.

Taylor Series Linearization Controller Comparison

Figure 13 and 14 shows the response of the LQG controller design, indicating the relative distance y over time. The solid black line indicates the response of the actual nonlinear system in the loop whereas the blue dotted line shows the response of the Taylor Series Linearized system. It is seen that the actual system goes unstable very quickly. This is because Taylor Series Linearization assumes that the system will be close to the equilibrium states, which is violated in the case of fairly large relative distances, which is considered.

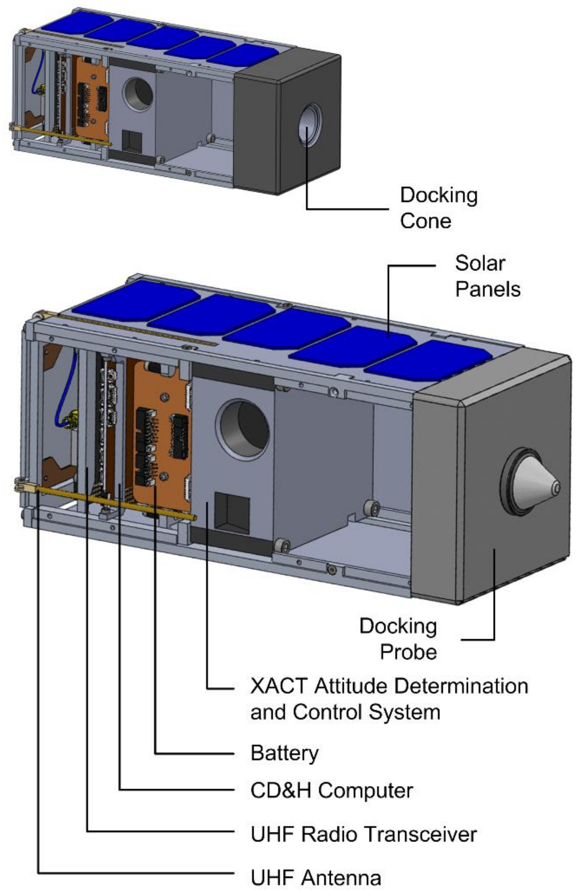

Figure 12: CAD Drawing of Docking Cone and Probe CubeSats.

Feedback Linearization Controller Comparison

Figure 15 shows the response of the LQG controller design, indicating the relative distance *y* over time. The solid black line indicates the response of the actual nonlinear system in the loop whereas the blue dotted line shows the response of the Feedback Linearized system. It is seen that the actual output deviates from the linearized system output but is stable. The system is stable because feedback linearization transforms the states and input so that no variation is lost in linearization. However, the large deviation in the system is because the controller design for the Feedback Linearized system is structured as a controller canonical representation and the controller designed cannot account for all the nonlinear variations that occur in the Feedback Linearized system. Figure 16 shows how the states of the

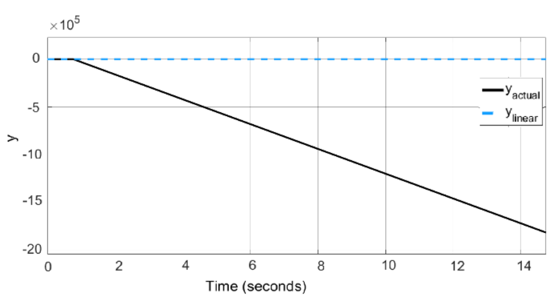

Figure 13: Taylor Series Linearization LQG Controller Theoretical vs. Actual y.

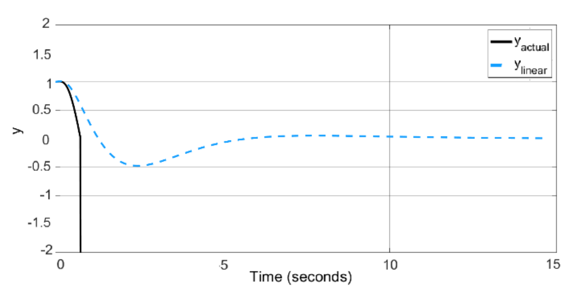

Figure 14: Taylor Series Linearization LQG Controller Theoretical vs. Actual y (Close-up).

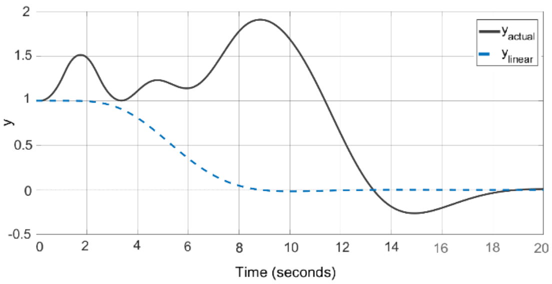

Figure 15: Feedback Linearization LQG Controller Theoretical vs. Actual y.

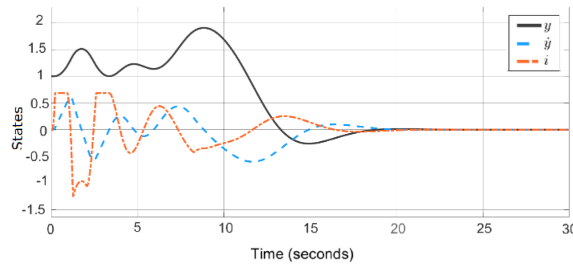

Figure 16: Feedback Linearization LQG Controller Actual States.

system vary over time. The solid black line indicates the relative position y over time, while the blue dotted line indicates the relative velocity $\dot{y}$ over time, and the dashed dotted orange line indicates the current in the electromagnetic coil i over time.

Distance compensated current control

From equation 3, if the distance between magnets is known, then the resulting force can be compensated for a known distance. The purpose of this technique is to provide an independent attraction (or repulsion) force so that a linear closed loop controller can be used for axial position and/or velocity. Given the amount of force requested, the current is then given by:

$$i_c = y\sqrt{\frac{F_c}{k}} \tag{6}$$

Where F_c and i_c are commanded force and the corresponding commanded current respectively. This can then be used to construct an axial velocity control system using:

$$F_c = -k_v(V - V_{ref}) \tag{7}$$

The resulting performance is displayed in figure 17, showing successful axial velocity control and docking occurring when the total position error is less than 2mm.

Simulation Results

The docking controller is interfaced with a simulation of the two small satellites orbiting around the Earth. Figure 18, 19 and 20 shows the fine docking system at three different instants of time, during the docking process.

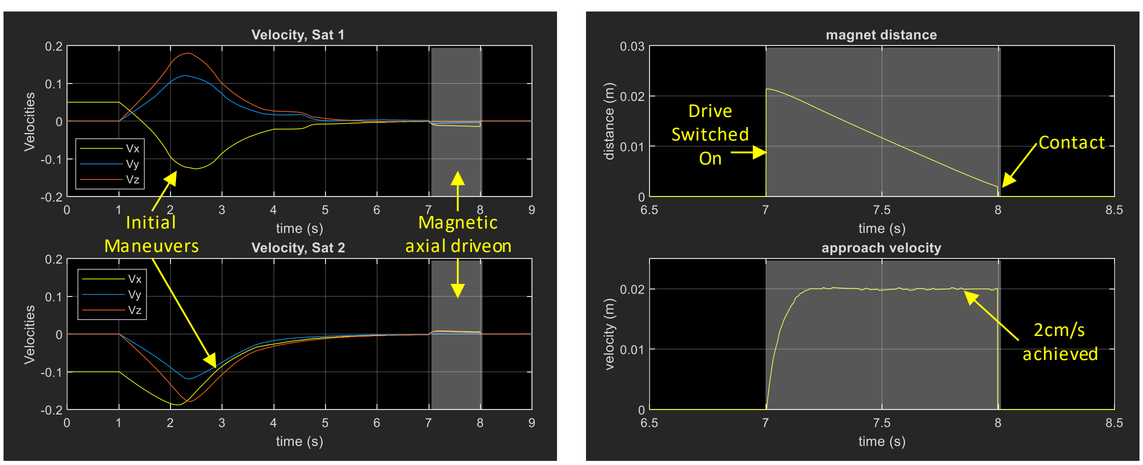

Figure 17: Simulation of docking sequence with magnetically controlled approach velocity

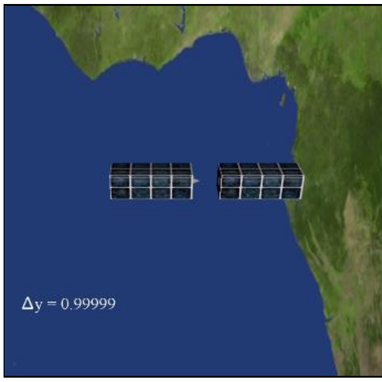

Figure 18: Docking System Simulation t_1.

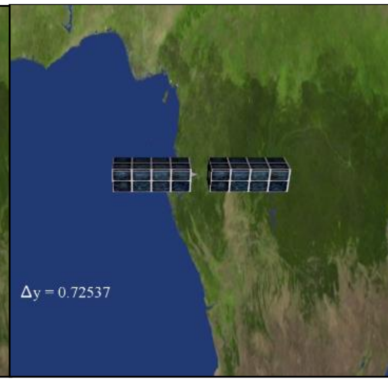

Figure 19: Docking System Simulation t_2.

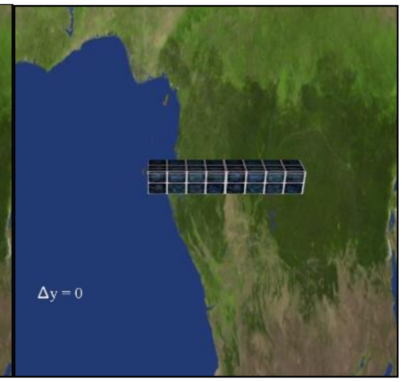

Figure 20: Docking System Simulation t_3.

It is seen from the controller design and the simulation that the docking system can successfully dock two small satellites from a given relative distance. It is important to note that the performance of this system depends on the parameter variations like k, R, L_1, and the voltage saturation limit included in the docking system model, indicative of the physical voltage limits of the power supply of the small satellite. For example, the maximum relative distance from which the fine docking system can dock two small satellites varies directly with the voltage saturation limit. If this limit is decreased, the max relative distance also decreases.

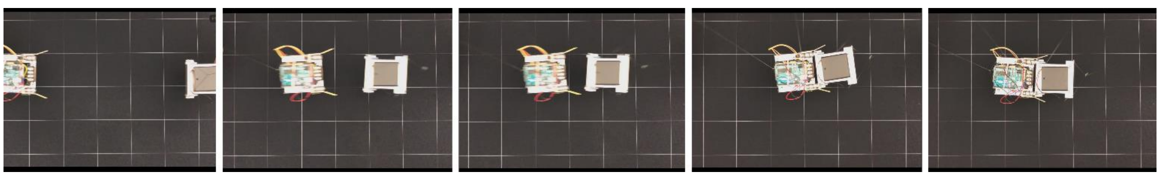

Figure 21: Docking demonstration in the laboratory. Time-lapsed photos over 0.6 seconds total.

HARDWARE DEMONSTRATIONS

In this section we present our efforts to build the electromagnetic docking system and test it in the laboratory (see Figure 21). One of the docking platforms has an electromagnet that is computer controlled and can be turned on or off using a Bluetooth radio transceiver. The other segment contains a block of steel. Each vehicle travels at nearly constant x and y velocity before making magnetic contact and finally docking as shown in figure 22. Docking takes place at 0.4 seconds.

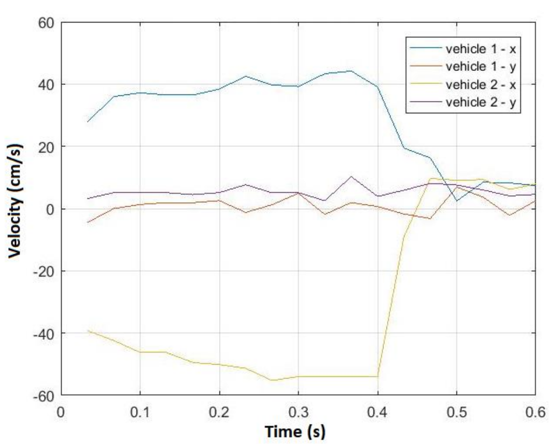

Figure 22: Velocities of the pair of docking vehicles.

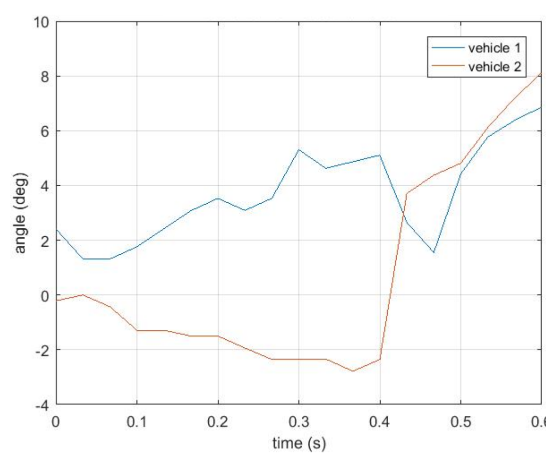

Figure 23: Relative angles of docking vehicles.

Upon docking, the two spacecraft are firmly in contact and aligned. One of the spacecraft has alignment appendages that simulates the cone and probe configuration. In addition, the spacecraft are also slightly misaligned based on Figure 23 which shows the orientation of both spacecraft as they are about to dock. The spacecraft at a maximum are 8-10 degrees misaligned. However, as the spacecraft is docking, their natural geometry forces alignment resulting in reduction. The is again shown by the sharp alignment in angle of the two vehicles after 0.4 seconds, followed by both crafts being aligned at 4 degrees and increasing in coordination. The slight increase in angles at the end is due to visual error of 1%. Figure 21 shows the relative x-position of the two crafts show the clear contact and docking at 0.4 s, while Figure 24 shows the relative-y position, while Figure 25 shows the relative y-position. We have performed the experiment repeatedly and found a docking success rate of 95 %. Our plans are afoot to do more extreme offset and adjusting of velocities to determine docking success.

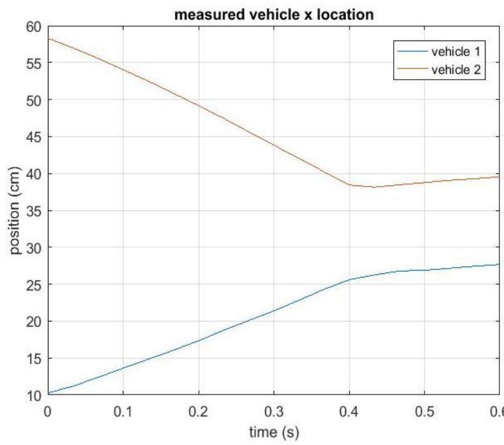

Figure 24: Relative x-positions

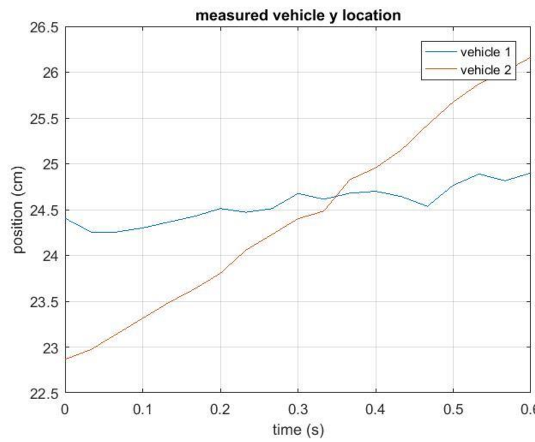

Figure 25: Relative y-positions

CONCLUSIONS

Docking systems enable in-space assembly and repair of large space structures. Introducing autonomy in the docking systems limits the use of highly skilled astronauts for what is otherwise a automatable task. Building small satellite docking systems enable small satellites to interact with large satellites by enabling resource sharing including computational power, data, electrical power and fuel. Small satellite docking systems have been designed but not been tested in space. With the development of a fine electromagnetic docking system shown here, it is possible to replace bulky sensors and cameras thereby allowing finer control over the docking process. This paper covers the modeling of an electromagnetic docking system using first principles and provided a comparison of fine docking controller designs. A simulation of the docking system was also shown. A mission for testing the docking system was proposed. Work is underway to model and test the variation in the performance of the system with parameter variations.

Experiments of the docking electromagnetic docking system has been carried out in the laboratory. The results show that docking is possible for relative velocities of 0.80 m/s. This is excellent news, as the system doesn't not require precision in point, velocities or position to enable docking. Further work will need to be done to better understand the failure scenarios for the electromagnetic docking system.

ACKNOWLEDGEMENTS

The authors would like to gratefully acknowledge Prof. Hugh Barnaby and Prof. Ashfaque Shafique from Arizona State University for their technical and mentoring support. The author would also like to thank the PhD students Himangshu Kalita and Aman Chandra of the SpaceTREx Laboratory at the University of Arizona for providing advice regarding the simulation design and CAD models of the CubeSats respectively.

REFERENCES

[1] A. Ravindran, "Small Satellite Electromagnetic Docking System Modeling and Control," M.S. thesis, Arizona State University, 2018.

[2] J. E. Krist and C. J. Burrows, "Phase-retrieval analysis of pre-and post-repair Hubble space telescope images," *Applied optics*, vol. 34, no. 22, pp. 4951-4964,1995.

[3] D. E. Hastings and C. Joppin, "On-orbit upgrade and repair: The hubble space telescope example," *Journal of spacecraft and rockets*, vol. 43, no. 3, pp. 614-625, 2006.

[4] E. W. Messerschmid and F. Renk, "Space stations," Wiley Online Library, 2010.

[5] S. R. Ellis, "Collision in space," *Ergonomics in Design*, vol. 8, no. 1, pp. 4-9, 2000.

[6] J. Cook, V. Aksamentov, T. Homan, and W. Bruner, "ISS interface mechanisms and their heritage," in AIAA SPACE 2011 conference & exposition, 2011, p. 7150.

[7] C. Unde7wood, S. Pellegrino, V. J. Lappas, C. P. Bridges, and J. Baker, "Using cubesat / micro-satellite technology to demonstrate the autonomous assembly of a reconfigurable space telescope (aarest)," *Acta Astronautica*, vol. 114, pp. 112-122, 2015.

[8] S. Eckersley, C. Saunders, D. Lobb, G. Johnston, T. Baud, M. Sweeting, C. Underwood, C. Bridges, and R. Chen, "Future rendezvous and docking missions enabled by low-cost but safety compliant guidance navigation and control (gnc) architectures," in Proceedings of The 15th Reinventing Space Conference. British Interplanetary Society, 2017.

[9] J. Bowen, M. Villa, and A. Williams, "Cubesat based rendezvous, proximity operations, and docking in the cpod mission," 2015.

[10] J. Griesbach, J.Westphal, C. Roscoe, D. Hawes, and J. Carrico, "Proximity operations nano-satellite flight demonstration (ponsfd) rendezvous proximity operations design and trade studies," in *Advanced Maui Optical and Space Surveillance Technologies Conference*, 2013.

[11] L. Rodgers, N. Ho, E. Jordan, M. Heiman, and D. Miller, "A universal interface for modular spacecraft," 2005.

[12] D. Miller, A. Saenz-Otero, J. Wertz, A. Chen, G. Berkowski, C. Brodel, S. Carlson, D. Carpenter, S. Chen, S. Cheng et al., "Spheres: a testbed for long duration satellite formation flying in micro-gravity conditions," in *Proceedings of the AAS/AIAA Space Flight Mechanics Meeting*, Clearwater, FL, Paper No. AAS 00-110, 2000.

[13] M. Barbetta, A. Boesso, F. Branz, A. Carron, L. Olivieri, J. Prendin, G. Rodeghiero, F. Sansone, L. Savioli, F. Spinello et al., "Arcade-r2 experiment on board bexus 17 stratospheric balloon," *CEAS Space Journal*, vol. 7, no. 3, pp. 347-358, 2015.

[14] J. Pei, L. Murchison, V. Stewart, J. Rosenthal, D. Sellers, M. Banchy, A. BenShabat, R. Elandt, D. Elliott, and A. K. Weber, "Autonomous rendezvous and docking of two 3u cubesats using a novel permanent-magnet docking mechanism," in *54th AIAA Aerospace Sciences Meeting*, 2016, p. 1465.

[15] D. W. Miller, S. Mohan, and J. Budino, "Assembly of a large modular optical telescope (almost)," in Space Telescopes and Instrumentation 2008: Optical, Infrared, and Millimeter, vol. 7010. *International Society for Optics and Photonics*, 2008, p. 70102H.

[16] R. McCormick, A. Austin, L. Cubrich, B. Marth, R. Mukherjee, T. Wenger, M. Patel, and K. Ho, "Development of miniature robotic manipulators to enable smallsat clusters," in Aerospace Conference, 2017 IEEE., 2017, pp. 1-15.

[17] D. Ye, Z. Yuan, L. Wen-juan, and T. Wenming, "Dynamic performance analysis of capture and separation process for a microsatellite docking device," *International Journal of Future Generation Communication and Networking*, vol. 8, no. 3, pp. 283-290, 2015.

[18] X. Zhang, Y. Huang, X. Chen, and W. Han, “Modeling of a space flexible probe-cone docking system based on the kane method,” *Chinese Journal of Aeronautics*, vol. 27, no. 2, pp. 248-258, 2014.

[19] Y. Qin, H. Peng, W. Ruan, J.Wu, and J. Gao, “A modeling and control approach to magnetic levitation system based on state-dependent arx model,” *Journal of Process Control*, vol. 24, no. 1, pp. 93-112, 2014.

[20] R. V. Gandhi and D. M. Adhyaru, “Feedback linearization based optimal controller design for electromagnetic levitation system,” in *Control, Instrumentation, Communication and Computational Technologies (ICCICCT*), 2016 International Conference on. IEEE, 2016, pp. 36-41.

[21] A. Romero Acero, J. A. Orozco Quiceno, J. Bulies, and J. Alberto, “Modelling and simulation of lqr and lfsv controllers in the magnetic levitation system (mls),” *Prospectiva*, vol. 14, no. 1, pp. 28-38, 2016.

[22] R. T. Nallapu, R. Furfaro, A. Ravindran, E. Asphaug, H. Kalita, J. Thangavelautham, and V. Reddy, “Smart camera system on-board a CubeSat for space-based object reentry and tracking,” *IEEE ION Plan Conference*, 2018.

[23] H. Kalita, A. Ravindran, J. Thangavelautham, “Exploration and Utilization of Asteroids as Interplanetary Communication Relays,” *Proceedings of the IEEE Aerospace Conference*, 2018.

[24] A. Chandra, J. Thangavelautham, “Modular Inflatable Space Structures,” *Proceedings of the IEEE Aerospace Conference*, 2018.